EXPLORATORY INVESTIGATION OF MULTIPLE MAPPING CLOSURE AS A MIXING MODEL IN LES-CMC

C.B. Devaud*, I. Stankovic, B. Merci****
cdevaud@uwaterloo.ca
*Department of Mechanical and Mechatronics Engineering, University of Waterloo
200 University Avenue West, Waterloo, Ont. Canada N2L 3G1.
** Ghent University - UGent, Department of Flow, Heat and Combustion Mechanics, Belgium.

Abstract
The scalar dissipation rate is a key quantity in turbulent combustion modelling, in particular for Conditional Moment Closure (CMC). Within the CMC framework, its conditional average at a particular value of mixture fraction is of special interest. The present study examines the deterministic version of Multiple Mapping Closure (MMC) to evaluate the conditionally filtered scalar dissipation rate in the filtered CMC equations in the context of Large Eddy Simulation (LES).
The objectives of the present investigation are (i) to use MMC to model the conditionally filtered scalar dissipation rate needed in LES-CMC and (ii) to determine if MMC is a viable option in the proposed framework. The paper presents our first results and focuses on the MMC equation, the role of each term in the MMC governing equation and the submodels needed.
One major scalar is selected, mixture fraction. The MMC transport equation is implemented in a LES code coupled with CMC to simulate a lifted jet flame in a vitiated coflow. At this initial stage of the present MMC study, it is useful to separate the MMC results and investigate the MMC operation and modelling alone before solving LES, CMC and MMC together. Thus, the MMC equation is solved starting from frozen flow, mixing and temperature fields. Discussion is focused on the models of the MMC unclosed terms and their impact on the prediction of the mapping function and the conditionally filtered scalar dissipation rate. The issue related to low levels of predicted subgrid variance in MMC compared to what is predicted in the LES solver is investigated.

Introduction

The scalar dissipation rate is a key quantity in turbulent combustion modelling, in particular for flamelet, Conditional Moment Closure (CMC) and Probability Density Function (PDF) approaches [1]. The scalar dissipation rate, N, represents the rate of mixing at the molecular level and is proportional to the mean square gradient of the scalar, Z, such as $N \equiv D\,\nabla Z \cdot \nabla Z$, where D is the molecular diffusivity of Z. Within the CMC framework, its conditional average at a particular value, η, of mixture fraction, Z is of special interest with $\langle N|\eta\rangle = \langle D\nabla Z \cdot \nabla Z|Z=\eta\rangle$. The angular brackets denote a conditional average over an ensemble of realizations of the flow, subject to the condition to the right of the vertical bar. Accurate modelling of the conditional scalar dissipation rate is crucial, as it appears in both the conditional species transport and temperature equations. However, evaluation of $\langle N|\eta\rangle$ is not straightforward. Further, CMC requires solution of the transport equations for the conditional averages to be consistent with that of the PDF transport equation [2]. When a presumed shape PDF is included, this condition can only be satisfied through the modelling of the conditional scalar dissipation rate derived from the PDF transport equation. Consequently, in cases of inhomogeneous turbulence, homogeneous mixing models do not provide closure for the conditional scalar dissipation rate that

preserves consistency with the inhomogeneous PDF transport equation. Two of the most commonly used models in CMC are the presumed β-PDF model of Girimaji [3] and Amplitude Mapping Closure (AMC) [4]. Both models are derived assuming homogeneous turbulence. Recently, Milford and Devaud [5] used a new formulation based on the transport equation of the mixture fraction PDF with different submodels for the conditional velocity in the case of high pressure autoignition. Predictions of ignition delay were significantly affected by the new inhomogeneous mixing formulation and in particular, the model for the conditional velocity was critical. These past simulations were carried out using Reynolds Averaged Navier Stokes (RANS) and very little has been investigated in the context of Large Eddy Simulation (LES). CMC has been used in LES only recently [6, 7, 8] and the AMC model is commonly used to determine the conditionally filtered scalar dissipation rate. In the present work, a different strategy is adopted to model the conditionally filtered scalar dissipation rate following promising research developments in Multiple Mapping Closure (MMC) [9, 10]. MMC methods have been developed using the concept of mapping closure [11]. In the simplest formulation, the mixture fraction can be selected as the only major species and MMC becomes equivalent to singly conditioned CMC. The advantage of MMC is that homogeneous turbulence is not assumed in the mapping process and as result, may be considered to be a generalization of AMC for inhomogeneous cases. Further, the conditionally filtered scalar dissipation rate is in closed form and no complex integration is needed as in the previous inhomogeneous turbulent mixing model [5].

The objectives of the present investigation are (i) to use MMC to model the conditionally filtered scalar dissipation used in CMC in LES and (ii) to determine if MMC is a viable option in the proposed framework. The paper presents our first results and focuses on the MMC implementation, the role of each term in the MMC governing equation and the submodels needed. Vogiatzaki et al.[9, 10] implemented MMC with a single major scalar, mixture fraction and calculated the unconditional and conditional scalar dissipation rate for simple jet flames. In the present work, same submodels are used with a different implementation in the context of LES where the calculations are three dimensional and transient by nature. To the authors' best knowledge, this is the first time the deterministic version of MMC is implemented in LES. The deterministic form is preferred in the present work in order to keep the additional computational cost low as the CMC equations are also solved for turbulent combustion. Further, the lifted hydrogen Cabra flame [12] is used as a test case with more challenging modelling aspects related to flame stabilization.

In the following sections, MMC is described including the modelling assumption used. The computational details of LES-CMC-MMC are shown. Results and discussion are focused on MMC submodels and their impact on the mapping function profiles in the computational domain.

MMC

A detailed derivation of MMC in both deterministic and stochastic forms can be found in the paper by Klimenko and Pope [11]. MMC is not straightforward and can become complex quickly depending on the number of major species or reference variables selected, the submodels (for example, for the velocity) and the equation formulation (deterministic versus stochastic). MMC is built upon the idea that all turbulent fluctuations can be divided into major and minor groups and turbulent fluctuations of minor scalars are correlated with those of the major scalars. A reference variable is assigned to each major scalar and the number of major scalars determines the dimensionality of the model. In the present work, keeping in mind the objective of finding the conditionally filtered scalar dissipation rate, one major scalar is selected, the conditioning variable used in CMC, namely mixture fraction. In other words, it is assumed that the fluctu-

ations of all other quantities that are called 'minor' in MMC, such as temperature and species concentrations are correlated to those of the major variable, mixture fraction. This is the same idea behind the singly conditioning CMC. The MMC equations solve for mapping functions which map between the reference space and the composition space following the same principle of mapping closure methods. The equations are derived for inhomogeneous turbulence and do not depend on the shape of the reference PDF. Further, the composition joint PDF can be determined directly from the solved mapping functions.

In the current work, the reference variable is noted as ξ. X_z is the mapping function solved by the MMC equation and X_z maps between ξ and Z, mixture fraction. The MMC equation for the spatial and temporal evolution of X_z is given by [11]

$$\frac{\partial X_z}{\partial t} + \mathbf{U}\nabla X_z + A\frac{\partial X_z}{\partial \xi} - B\frac{\partial^2 X_z}{\partial \xi^2} = 0, \tag{1}$$

where $\mathbf{U}$, A and B are the coefficients of velocity, drift and diffusion, respectively, and need to be closed. Closure of these terms is obtained through consistency with the reference PDF transport equation. A Gaussian form with zero mean and unity variance is commonly used for the reference PDF, P_ξ, and satisfies the following transport equation

$$\nabla \mathbf{U}\overline{\rho}P_\xi + \frac{\partial A\overline{\rho}P_\xi}{\partial \xi} + \frac{\partial^2 B\overline{\rho}P_\xi}{\partial \xi^2} = 0, \tag{2}$$

where $\overline{\rho}$ is the filtered density. Please note that the time and spatial derivatives are neglected in Eq. 2 due to time and space invariance of the reference PDF. Further, the reference PDF does not have to be Gaussian and the coefficients can be determined in principle for any form of reference PDF. However, the choice of the reference PDF has an impact on the resulting complexity for the expressions of $\mathbf{U}$ and A and influences the implementation of MMC.

All MMC coefficients must satisfy Eq. 2. However, it does not mean that they are unique [11]. Their expressions depend on the assumptions made for the velocity and B. For our first MMC implementation, models suggested by Klimenko and Pope [11] and implemented in RANS by Vogiatzaki et al. [9, 10] are used in the present work. For clarity, the MMC velocity denotes $\mathbf{U}$, the velocity vector, in Eq. 1, whereas the term 'conditional velocity' is kept for the velocity in the CMC equations. Both are conditional velocities but are not conditioned on the same variable. A linear model is used for $\mathbf{U}$ given by

$$\mathbf{U} = \mathbf{U}(\xi, \mathbf{x}, t) = \mathbf{U}^{(0)} + \mathbf{U}^{(1)}\xi, \tag{3}$$

$\mathbf{U}^{(0)}$ corresponds to the filtered velocity vector solved in LES, such as

$$\mathbf{U}^{(0)} = \tilde{\mathbf{U}}. \tag{4}$$

$\mathbf{U}^{(1)}$ is the velocity gradient and is determined by the expression

$$\mathbf{U}^{(1)}\langle \xi X_z \rangle^* = \widetilde{\mathbf{u}'Z'}, \tag{5}$$

where Z is the mixture fraction modelled by the mapping function such as Z=$\langle X_z \rangle^*$. In the context of LES, the terms with overtilde are filtered/resolved quantities and terms in angular brackets with a star are averages obtained using the reference PDF. The drift coefficient is determined by

$$A = -\frac{\partial B}{\partial \xi} + B\xi + \frac{1}{\overline{\rho}}\nabla\overline{\rho}\mathbf{U}^{(1)}. \tag{6}$$

B is related to the unconditional scalar dissipation rate and is modelled as

$$B\langle\frac{\partial X_z}{\partial \xi}\frac{\partial X_z}{\partial \xi}\rangle^* = \tilde{N}. \tag{7}$$

Equations 3-5 imply that B can be treated as an independent coefficient [9]. This is common practice as shown in [11]. Equation 7 requires knowledge of $\tilde{N}$ obtained from LES which includes contribution of resolved and subgrid gradients and is calculated as

$$\tilde{N} = \left(\frac{\nu}{Sc} + \frac{\nu_t}{Sc_t}\right)\frac{\partial \widetilde{Z}}{\partial x_k}\frac{\partial \widetilde{Z}}{\partial x_k}, \tag{8}$$

where ν is the molecular kinematic viscosity, ν_t the turbulent viscosity, Sc is the molecular Schmidt number and Sc_t the turbulent Schmidt number. The conditionally filtered scalar dissipation rate, needed in CMC, does not appear explicitly in the MMC formulation. It can be retrieved through a transformation from the reference space, ξ, to the mixture fraction space, η, such that [9, 10]

$$\widetilde{N|\eta} \approx B\left(\frac{\partial X_z}{\partial \xi}\right)^2. \tag{9}$$

Experimental details

The selected experimental case is a turbulent lifted jet flame of hydrogen diluted with nitrogen issuing into a wide co-flow of vitiated air [12]. As shown in Fig. 1, the burner consists of a fuel jet nozzle and a surrounding perforated plate disk. The jet nozzle inner diameter, d, is $4.57\ \mathrm{mm}$ and the wall thickness is $0.89\ \mathrm{mm}$. The outer disk has a diameter of $210\ \mathrm{mm}$ with an 87% blockage and consists of 2200 holes with a diameter of $1.58\ \mathrm{mm}$. The central jet extends $70\ \mathrm{mm}$ above the surface of the perforated disk. At this downstream location the co-flow properties are uniform. The fuel stream consists of hydrogen diluted with nitrogen. The vitiated air consists of the products of a lean premixed hydrogen/air flame. The stoichiometric mixture fraction is 0.474. The experimental conditions used in the present simulations are summarized in Table 1.

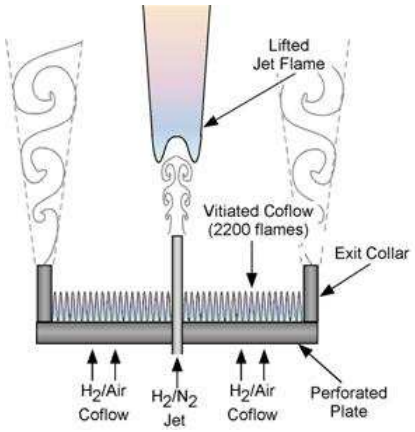

Figure 1: Experimental set-up taken from http://www.me.berkeley.edu/cal/vcb/data/VCHNData

Table 1: Experimental conditions

	co-flow	fuel jet
Diameter (mm)	4.57	210
Velocity (m/s)	107	3.5
Temperature (K)	1045	305
X_{H_2} (molar fraction)	0.0005	0.2537
X_{O_2} (molar fraction)	0.1474	0.0021
X_{N_2} (molar fraction)	0.7534	0.7427
X_{H_2O} (molar fraction)	0.0989	0.0015

Computational details for LES

For brevity, the governing equations and models are not presented in full detail and further information can be found in [8]. The LES with the first-order CMC approach and detailed mechanism including 9 species and 19 reversible reactions [13], is used for the flow calculations. The flow field information is calculated by the LES code [8]. The standard Smagorinsky model is used to calculate the sub-grid scale stress tensor with a model constant, C, equal to 0.1. Equal diffusivities, constant Schmidt number ($Sc = Sc_t = 0.7$) and unity Lewis number are applied. No additional equation is solved for the subgrid mixture fraction variance. A gradient type model is considered such that

$$\widetilde{Z''^2} = C\Delta^2 \frac{\partial \widetilde{Z}}{\partial x_k} \frac{\partial \widetilde{Z}}{\partial x_k}, \tag{10}$$

where Δ is the filter width and x_k corresponds to distance in each direction of the selected co-ordinate system.

The LES computational domain extends 30 d downstream from the jet inlet (approximately 137mm) in the axial direction and 20 d (91.4mm) radially. The corresponding grid contains 192 $\times$ 48 $\times$ 48 cells. The LES grid is stretched smoothly towards the co-flow in the radial direction and is expanded smoothly in the axial direction. At the inlet of the domain, Dirichlet boundary conditions are used imposing the velocity and mixture fraction. At the outlet, Neumann boundary conditions are applied for all quantities except for pressure which is imposed (atmospheric pressure). The implementation is in parallel with 4 blocks in the axial direction.

CMC formulation in LES

The conditionally filtered CMC equations are given by

$$\frac{\partial Q_\alpha}{\partial t} + \underbrace{\widetilde{\mathbf{u}|\eta} \cdot \nabla Q_\alpha}_{T_1} - \underbrace{\widetilde{N|\eta} \frac{\partial^2 Q_\alpha}{\partial \eta^2}}_{T_2} = \underbrace{\widetilde{\omega_\alpha|\eta}}_{T_3} + \underbrace{e_Y}_{T_4}, \ \alpha = 1, ..., n \tag{11}$$

where $Q_\alpha = \widetilde{Y_\alpha|\eta}$ represents the conditionally filtered mass fraction of the α-species, $\widetilde{\mathbf{u}|\eta}$ is the conditionally filtered velocity and $\widetilde{\omega_\alpha|\eta}$ the conditionally filtered chemical source term. The variable η is the sample space variable for Z (mixture fraction) and the operator $\cdot|\eta$ denotes fulfillment of the condition on the right hand side of the vertical bar. The conditional fluctuations around the conditional mean are neglected in the present first order CMC. The equations are

solved for the n species of the reaction mechanism. The first term on the left-hand side of Eq. 11 is the unsteady term. The second term represents the transport by convection (T1). The last term on the left-hand (T2) side represents diffusion in mixture fraction space, i.e. the conditionally filtered scalar dissipation rate term. The first term on the right-hand side (T3) is the conditional chemical source term, determined using first order closure. The last term on the right-hand side (T4) accounts for the conditional transport in physical space and is modeled using the gradient approach: $e_{_Y} = -\frac{\nabla\cdot(\bar{\rho}\widetilde{\mathbf{u}''Y''_\alpha}|\eta\widetilde{P}(\eta))}{\bar{\rho}\widetilde{P}} \approx \frac{1}{\bar{\rho}\widetilde{P}(\eta)}\frac{\partial}{\partial x_i}[\overline{\rho}\widetilde{P}(\eta)D_t^*\frac{\partial Q_\alpha}{\partial x_i}]$, where D_t^* is the sub-grid scale turbulent diffusivity. To obtain complete closure of Eq. 11, models are required for $\widetilde{N|\eta}$, D_t^* and $\widetilde{u_i|\eta}$.

The conditionally filtered scalar dissipation rate is determined by AMC [4] using

$$\widetilde{N|\eta} = \frac{\widetilde{N}G(\eta)}{\int_0^1 \widetilde{P}(\eta)G(\eta)d\eta}, \tag{12}$$

where $\widetilde{N}$ is the sum of the resolved and the sub-grid scale unconditional scalar dissipation rate, as shown in Eq. 8. AMC always provides $\widetilde{N|\eta}$ as function of mixture fraction is prescribed by the bell-shape of function $G(\eta) = exp(-2[erf^{-1}(2\eta - 1)]^2)$. This is the ultimate objective of the present study to substitute the AMC expression, Eq. 12 by the MMC formulation given by Eq. 9.

In CMC, the equations for the species mass fractions and temperature are solved, based on which the conditional density is calculated. Integration with the filtered β PDF over mixture fraction space yields the unconditional density, temperature and species mass fractions. The LES and CMC solvers are coupled and the information from CMC is transferred at every timestep of the simulation to the LES in order to update flow field.

A coarser spatial mesh is used to solve the CMC equations discretized in finite differences. The CMC grid consists of 80 $\times$ 5 $\times$ 5 cells where the domain is also divided into 4 blocks in the axial direction. The mixture fraction is discretized into 50 bins, clustered around the most reactive mixture fraction approximately equal to 0.06. Information is transferred from the finer LES spatial mesh to the coarser CMC grid using volume averaging. For conditional scalar dissipation rate, the AMC model is applied directly to the CMC cells in order to obtain $\widetilde{N|\eta}$. The density-weighted filtered PDF ($\widetilde{P}(\eta)$) is assumed to have a β-shape on the CMC mesh. The conditional turbulent velocity and diffusivity used in CMC are calculated by

$$\widetilde{u_i|\eta} = \frac{\int \widetilde{u}_i\bar{\rho}dV}{\int \bar{\rho}dV}|_{CFD\in CMC} \quad \text{and} \quad D_t^* = \frac{\int D_t\bar{\rho}dV}{\int \bar{\rho}dV}|_{CFD\in CMC}, \tag{13}$$

respectively, where $\widetilde{u}_i$ is the filtered velocity in the ith direction, D_t turbulent diffusivity (on fine LES mesh) and dV the elemental volume.

MMC implementation

Due to increased memory allocation and our current computational system, the MMC equation, Eq. 1, can only be solved in two spatial dimensions: the axial (y axis) and radial (z axis) directions are kept. The centre plane is selected from the LES 3D domain and the LES mesh resolution is maintained with the parallel implementation. 53 nodes are used to cover the reference space variable, ξ for the interval [-4,4] clustered around ξ=0. A fractional step method is

applied: Eq. 1 is split into two ODEs (Eqs.14 and 15) following

$$\frac{\partial X_z}{\partial t} = \underbrace{-\mathbf{U}\nabla X_z}_{\text{transport in space}} \quad , \tag{14}$$

$$\frac{\partial X_z}{\partial t} = \underbrace{A\frac{\partial X_z}{\partial \xi} - B\frac{\partial^2 X_z}{\partial \xi^2}}_{\text{transport in } \xi \text{ space}}. \tag{15}$$

The ODE including spatial transport is non-stiff and is solved using first-order explicit Euler method. The second ODE considers transport in ξ space and is solved using the VODPK solver [14]. Boundary conditions are defined in both physical and reference spaces. Second order central differencing scheme is used for the discretization of diffusion terms, a second order Total Variation Diminishing (TVD) scheme [15] for the spatial convective term and hybrid scheme for convection in ξ space. At the inlet (i.e. $y = 0$), Dirichlet boundary conditions are used. At the outlet ($y = 30d$) and at both ends in the z direction, i.e. $z = -10d$ and $z = 10d$, zero gradient is imposed. In ξ space, at $\xi = -4$ and $\xi = 4$ zero gradient is imposed. Values of $\mathbf{U}$, A and B are calculated explicitly based on the solution at the previous iteration.

Initializations of X_z as a function of ξ are crucial in order to introduce the right amount of "fluctuations" in the calculations. At every point in space, initializations are carried out in order to conserve the first and second moments of Z such as

$$\tilde{Z} = \langle X_z \rangle^* = \int_{-\infty}^{\infty} X_z P_\xi d\xi, \tag{16}$$

$$\widetilde{Z''^2} = \langle X_z' \rangle^* = \int_{-\infty}^{\infty} (X_z - \langle X_z \rangle^*) P_\xi d\xi. \tag{17}$$

Results

First, LES and CMC are run for 80000 time steps, i.e. 20 ms, with each time step being equal to $\Delta t_{LES} = 2.5 \times 10^{-7}$ s in order to have well-established burning conditions in the domain. The LES-CMC results for the same flame are reported in a different paper [16]. The predicted lift-off height, temperature and species concentrations are shown to be in very good agreement with experimental data. Thus, the present LES-CMC data provides excellent basis for the MMC investigation. The MMC results shown thereafter are obtained starting from these frozen flow, mixing and temperature fields. For illustration, Figure 2 gives the instantaneous temperature contours at 20 ms provided by LES-CMC and used as initial data for MMC. There is no issue in the MMC-LES-CMC coupling. Note that MMC does not have any direct effect on the flow and mixing fields, the link between MMC and CMC is through the determination of the conditionally filtered scalar dissipation using Eq. 9. At this initial stage of the present MMC study in LES-CMC, it is useful to separate the MMC results and investigate the MMC operation and modelling alone before solving LES, CMC and MMC together. In order to examine the profiles of mapping function and resulting conditional scalar dissipation rate, two points are selected in the computational domain. Their coordinates are shown in Table 2. The values of $\tilde{Z}$ and $\widetilde{Z''^2}$ are also included in Table 2 as these have a direct impact on the shape of the mapping function, X_z. These two points are also indicated in Fig. 2. Points 1 and 2 demonstrate relative high level of subgrid fluctuations. Consequently, their respective mapping functions are expected to represent a large range of mixture fraction values. Figure 3 a) and b) shows the initial values of X_z and values obtained after solving the MMC equation for 2200 time steps, i.e 0.55 ms, for point 1 and 2, respectively. As can be seen, the mapping functions did change in reference

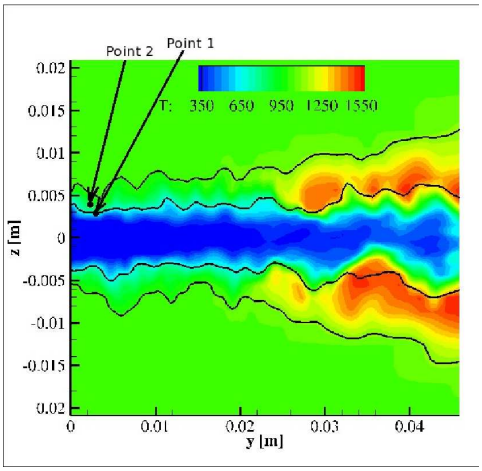

Figure 2: Instantaneous temperature contours at 20 ms

Table 2: Specifications of Point 1 and 2

	Point 1	Point 2
axial location, y (mm)	2.92	2.46
radial location, z (mm)	2.99	3.87
$\tilde{Z}$ from LES	0.864	0.265
$\widetilde{Z''^2}$ from LES	0.88×10^{-2}	0.767×10^{-2}

space, whereas the mixing and velocity fields did not. In particular, X_z has the tendency to become flatter resulting in lower subgrid fluctuations predicted by MMC. Using Eqs 16 and 17, after 2200 time steps, at point 1 the calculated value for $\tilde{Z}$ and $\widetilde{Z''^2}$ is 0.743 and 0.566×10^{-2}, respectively. At point 2, the MMC recovered values are 0.149 for $\tilde{Z}$ and 0.553×10^{-4} for $\widetilde{Z''^2}$ after 2200 time steps. These are to be compared with the initial values equal to the LES data shown in Table 2. A discrepancy can be seen for $\tilde{Z}$ on the order to 14% and 43% for point 1 and 2, respectively. This difference in the MMC predicted $\tilde{Z}$ is a consequence of the low generated fluctuations in Z: at point 1, the sugbrid variance is underpredicted by 36%, whereas the predicted subgrid fluctuations are more than 100 times smaller than expected at point 2. When there is no fluctuation generated by the MMC velocity, the mapping function becomes flat and constant in reference space tending to the filtered mixture fraction, $\tilde{Z}$. This is observed, for example, when the term including the velocity gradient and turbulent flux, Eq. 5, is neglected. Our preliminary test calculations confirmed this was the case, consistent with previous results [9, 10]. The mapping functions are initialized using Eqs. 16 and 17. Thus, no change would be expected for the present "frozen" mixing and flow conditions. The underprediction of subgrid fluctuations is also shown in Fig. 4 a) where the radial profile of the MMC predicted rms is compared with the LES values at $y = 2.46$ mm. The MMC subgrid fluctuation profile is narrower and lower in magnitude compared to the LES values. Figure 4 b) also confirms the same trend on the centreline in the entire domain. However, the subgrid fluctuation level is well captured for distances up to 13d with decreasing level further downstream.

The possible sources of discrepancy can be either due to (i) numerical errors and/or due to (ii) the selected submodels. In term of numerical implementation, the MMC equations are

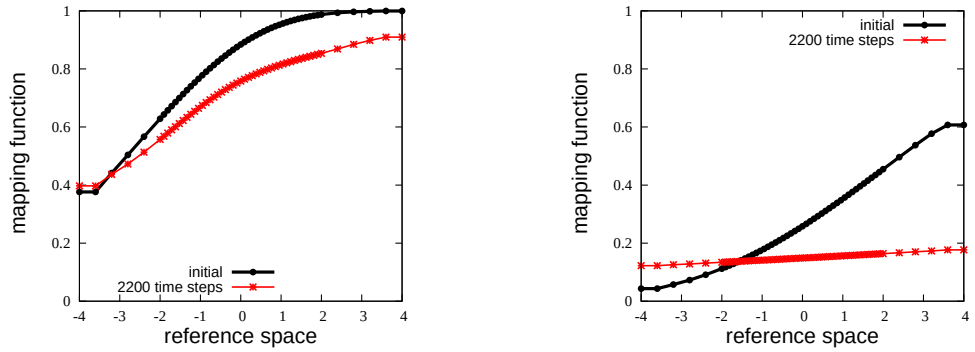

(a) Point 1 (b) Point 2

Figure 3: Mapping function in reference space, ξ

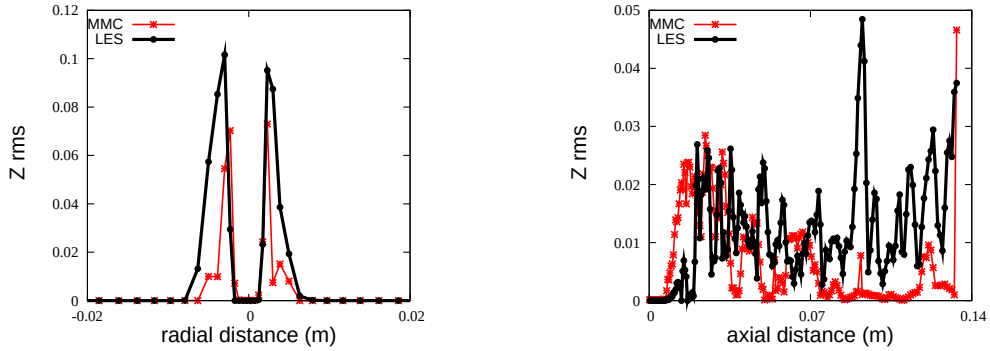

(a) radial profile at y=2.46 mm (b) centreline profile

Figure 4: Profiles of MMC predicted fluctuations compared with LES results. $Z_{rms} = \sqrt{\widetilde{Z''^2}}$ and MMC values are obtained using Eq. 17

solved in two physical dimensions instead of three in the LES flow equations. It is difficult to quantify this discrepancy, however, spatial transport in the circumferential direction is expected to be much smaller than that in the other two (i.e. axial and radial) directions. Spatial transport is discretized using the TVD scheme in MMC and LES, which is a second order approximation. The fractional step method may be sensitive to the time step and number of steps. Throughout our tests, the local MMC time step is shown to have a significant impact on the MMC solution. This is also due to first order and explicit formulation of the transient term in Eq. 1. Further, as shown in Fig. 5, the two dominant terms in Eq. 1 are the two convective terms, one in physical space and one in reference space. In all cases, diffusion appears to be much lower. This observation on the MMC equation budget is in agreement with the findings of Vogiatzaki et al. [9, 10]. The local time step is varied successively until no significant difference is noticed in the mapping function profiles. The present local time step corresponds to $\Delta t_{LES}/200 = 1.25 \times 10^{-9}$ s. A higher value of $\Delta t_{LES}/100$ also works and may have to be selected for future calculations to save computational time. Qualitatively, the MMC equation and the resulting mapping functions behave in a consistent manner according to what is reported by previous MMC studies [9, 10]. Further improvements to the current implementation may still be possible. However, after many tests and verifications, the observed discrepancy in the subgrid fluctuation level in MMC is likely to be related to some modelling aspects, in particular, the fluctuation generation mechanism in MMC. This points towards the linear model for the MMC velocity.

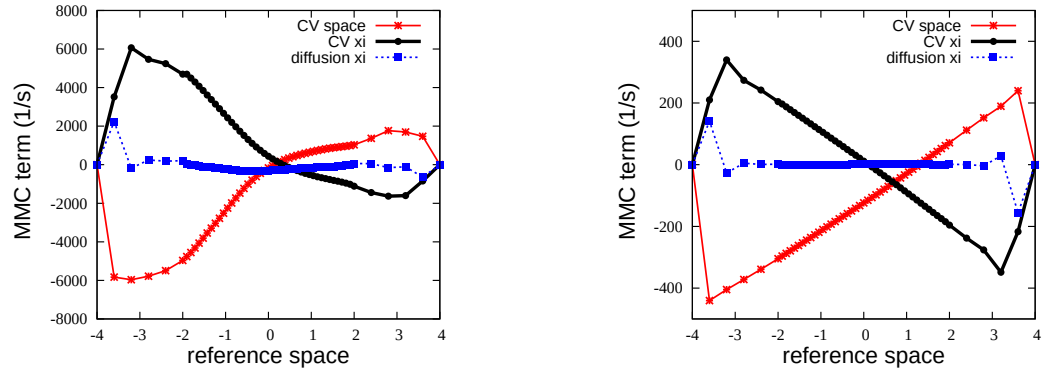

(a) Point 1 (b) Point 2

Figure 5: MMC budget in Eq. 1 after 2200 time steps, 'CV space' corresponds to the right-hand side (rhs) of Eq. 14, 'CV xi' first term of rhs in Eq.15 and 'diffusion xi' second term of rhs of Eq. 15

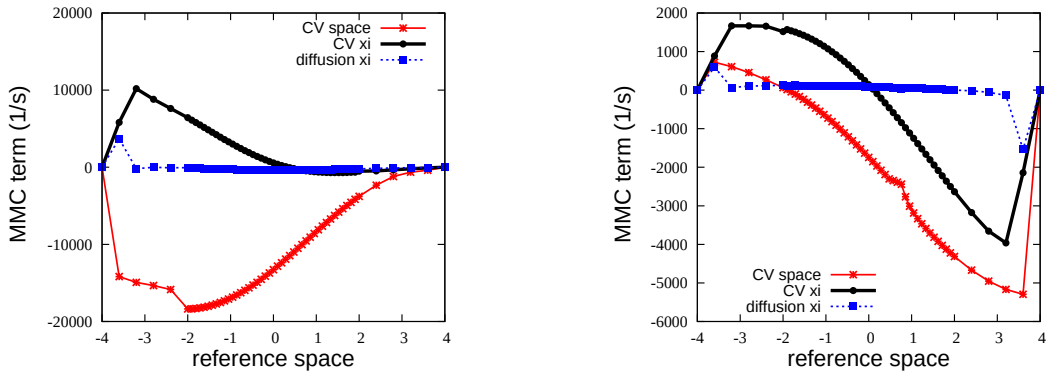

(a) Point 1 (b) Point 2

Figure 6: MMC budget in Eq. 1 after 1 time step, 'CV space' corresponds to the right-hand side (rhs) of Eq. 14, 'CV xi' first term of rhs in Eq. 15 and 'diffusion xi' second term of rhs of Eq. 15

The fluctuations are only introduced through Eq. 5 in MMC and any modelling inaccuracies in the MMC velocity have a direct impact on the calculation of A. According to the initial MMC budget shown in Fig. 6a), at Point 1, balance is not completely achieved between the two convective terms. However these two terms have opposite signs and can be seen to reach a balance within minor adjustments. However, in Fig. 6b), the same budget at Point 2 reveals a very different picture with both convective terms being of the same sign for positive values of ξ. As a result they cannot balance each other without drastic changes in the mapping function profiles. At this stage, further investigation is required to understand why the linear model produces more reasonable values at some positions but incorrect at other positions.

Figure 7 shows the profiles of the conditionally filtered scalar dissipation rate using AMC (homogeneous turbulent model), MMC from the initial values and MMC after 2200 time steps at points 1 and 2. It is clear that the MMC shapes are significantly different from the AMC values. The MMC predictions are not centered on a mixture fraction of 0.5. In Fig. 7 a), the initial MMC profile is close to AMC for mixture fractions larger than 0.5 but shows a cutoff around 0.4 where no mixing takes place between 0 and 0.4 in agreement with the lowest value of X_z in Fig. 3. This difference is expected to have an impact on the CMC calculations, which needs to be

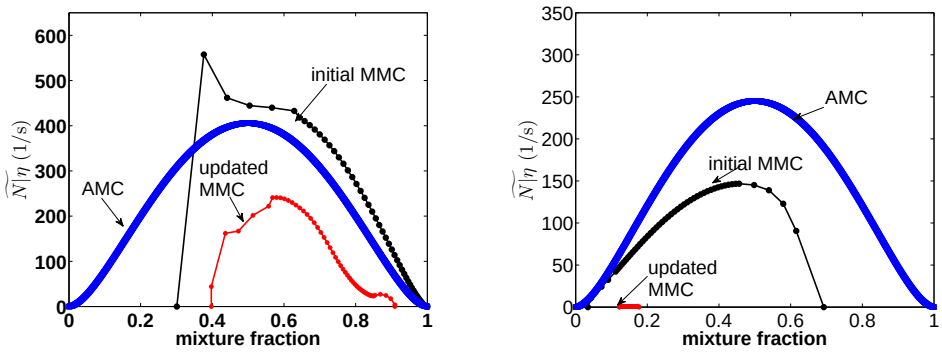

(a) Point 1 (b) Point 2

Figure 7: Conditionally filtered scalar dissipation rate, initial MMC means values calculated from the initial mapping function profiles, updated MMC values determined after 2200 time steps, AMC values calculated using Eq. 12

evaluated in future work. As can be seen in Fig. 7 b), initial MMC and AMC values are in close agreement for very small values of η. Initial MMC always produces values lower than those of AMC, in particular for mixture fraction values larger than 0.1. The discrepancy in the predicted level of fluctuations (after 2200 time steps) has the effect of lowering the magnitude of the scalar dissipation rate. In particular, at point 2, the subgrid fluctuations are severely underpredicted in MMC resulting in very small value of N. Thus, it appears important to reproduce the correct LES values in MMC before moving to the fully coupled LES-CMC-MMC.

Conclusions

A first implementation of MMC as a mixing model was studied within the framework of LES-CMC. As a first step, MMC was applied to "frozen" mixing and flow conditions from initial LES-CMC simulations. It was shown that the level of subgrid fluctuations predicted by MMC was lower than that obtained in LES. This discrepancy may stem from the numerical implementation and/or the submodels used in MMC. Without excluding entirely possible numerical aspects, issues related to the modelling of the MMC velocity are more likely to be the explanation. The validity of the linear model for conditional velocity is questionable [5, 9, 10] and other closures are currently being investigated. The resulting conditionally filtered scalar dissipation rate is significantly different in shape and magnitude compared to the AMC values. It is also sensitive to the predicted MMC level of fluctuation. Thus, it is crucial to get the correct level of fluctuations in MMC before moving to the next step, running fully coupled LES-CMC-MMC and evaluate the impact of the newly modelled conditionally filtered scalar dissipation rate on the prediction of lift-off height, species concentration and temperature.

Acknowledgements

The authors would like to thank Dr. K. Vogiatzaki for helpful discussions on MMC.

References

[1] R.O. Fox. *Computational models for turbulent reacting flows*. Cambridge University Press, 2003.

[2] A.Y. Klimenko and R.W. Bilger. Conditional moment closure for turbulent combustion. *Prog. Energy Combust. Sci.*, 25(6):595–687, 1999.

[3] S.S. Girimaji. On the modeling of scalar diffusion in isotropic turbulence. *Phys. Fluids A*, 4(11):2529–2537, 1992.

[4] E. O'Brien and T.L. Jiang. The conditional dissipation rate of an initially binary scalar in homogeneous turbulence. *Phys. Fluids A*, 3(12):3121–3123, 1991.

[5] A. Milford and C.B. Devaud. Investigation of an inhomogeneous turbulent mixing model for conditional moment closure applied to autoignition. *Combust. Flame*, 157:1467–1483, 2010.

[6] S. Navarro-Martinez and A. Kronenburg. LES-CMC simulations of a lifted methane flame. *Proc. Combust. Inst.*, 32:1509–1516, 2009.

[7] A. Triantafyllidis, E. Mastorakos, and R.G.L.M Eggels. Large eddy simulations of forced ignition of a non-premixed bluff-body methane flame with conditional moment closure. *Combust. Flame*, 156:2328–2345, 2009.

[8] I. Stankovic, A. Triantafyllidis, E. Mastorakos, C. Lacor, and B. Merci. Simulation of hydrogen auto-ignition in a turbulent co-flow of heated air with LES and CMC approach. *Flow, Turbulence and Combustion*, 86:689–710, 2011.

[9] K.Vogiatzaki, A.Kronenburg, M.J.Cleary, and J.H.Kent. Multiple mapping conditioning of turbulent jet diffusion flames. *Proc. Combust. Inst.*, 32:1679–1685, 2009.

[10] K.Vogiatzaki, M.J.Cleary, A.Kronenburg, and J.H.Kent. Modeling of scalar mixing in turbulent jet flames by multiple mapping conditioning. *Phys. Fluids*, 21:025105, 2009.

[11] A.Y.Klimenko and S.B. Pope. A model for turbulent reactive flows based on multiple mapping conditioning. *Phys. Fluids*, pages 1907–1925, 2003.

[12] R. Cabra, T. Myhrvold, J.Y. Chen, R.W. Dibble, A.N. Karpetis, and R.S. Barlow. Simultaneous laser raman-rayleigh-lif measurements and numerical modelling results of a lifted turbulent H_2/N_2 jet flame in a vitiated co-flow. *Proc. Combust. Inst.*, 29:1881–1888, 2002.

[13] J. Li, Z. Zhao, A. Kazakov, and F. L. Dryer. An updated comprehensive kinetic model of hydrogen combustionxs. *Inter. J. Chem. Kinet.*, 36:566–575, 2004.

[14] P. N. Brown and A. C. Hindmarsh. Reduced storage matrix methods in stiff ode systems. *J. Comput. Appl. Math.*, 31:40–91, 1989.

[15] B. Van Leer. Towards the ultimate conservative difference scheme ii. monotonicity and conservation combined in a second order scheme. *J. Comput. Phys.*, 14:361–370, 1974.

[16] I. Stankovic and B. Merci. LES-CMC simulations of turbulent hydrogen flame in a vitiated air co-flow. *Submitted to MCS7*, pages 1–12, 2011.